Thermal Equilibrium between Quinoid/Biradical Forms Enhancing Electrochemical Amphotericity

Yusuke Ishigaki,*[a] Shin-ichi Mizuno,[a] Kazuma Sugawara,[a] Takumi Hashimoto,[a] Shuichi Suzuki,[b] and Takanori Suzuki*[a]

Abstract: Upon dibenzo annulation on Thiele's hydrocarbon (tetraphenyl-*p*-quinodimethane), the quinoid form and the biradical form adopt quite different geometries, and thus are no longer resonance structures. When these two forms can interconvert rapidly due to the small energy barrier ($\Delta G^{\ddagger}$), the equilibrated mixture contains both forms in a ratio that is determined by the energy difference (ΔG^{o}) between the two forms. For a series of tetrakis[5-(4-methoxyphenyl)-2-thienyl]-substituted derivatives, the more stable quinoid form and the metastable biradical form coexist in solution as an equilibrated mixture due to small $\Delta G^{\ddagger}$ (< 15 kcal mol^{-1}) and ΔG^{o} (1-4 kcal mol^{-1}), in which the proportion of the two forms can be regulated by temperature. Since the biradical form can undergo easy two-electron (2e) oxidation to the corresponding dications as well as easy 2e reduction to the dianions, it exhibits very high electrochemical amphotericity. This character with a record-small span for not only the first oxidation and reduction potentials but also the second those, [$E_1^{sum} \approx E_2^{sum} = E_2^{ox} - E_2^{red}$ = ca. 1.4 V], is attained through thermally enhanced conversion to the biradical form from the corresponding quinoid form, the latter of which is less amphoteric due to higher E^{ox} and lower E^{red} values.

Introduction

p-Quinodimethanes are representative non-aromatic π-conjugated systems that are found in many organic redox-active skeletons.[1] For example, when amino[2] or cyano[3] groups are attached at exocyclic bonds (**I$_{NR2}$** and **I$_{CN}$**), they facilely undergo electrochemical oxidation or reduction, respectively, accompanied by the formation of a planar aromatic sextet (Scheme 1a), which supports their easy electron transfer as well as stabilization of the resulting charged species. Such molecules are sufficiently stable in the uncharged state, compared to the parent *p*-quinodimethane[4] which exhibits high reactivity to convert oligomers/polymers.

When bulky but electronically neutral groups (e.g., phenyl) are attached at exocyclic bonds, considerable stability is also attained, as demonstrated by tetraphenyl-*p*-quinodimethane (Thiele's hydrocarbon, **II-A**),[5] which is still susceptible to light and oxygen due to its expected biradical character (**II-B**) (Scheme 1b). The resonance structure of **II-A** and **II-B** is one of the fundamental units found in many singlet biradicaloid molecules, such as indenofluorene (**III-A**/**III-B**)[6] or fused-bis(phenalenyl) (**IV-A**/**IV-B**)[7,8] (Scheme 1c).

On the other hand, a quite different scenario is expected when two benzene nuclei are fused to Thiele's hydrocarbon, as in 9,10-anthraquinodimethanes (**V-A**) (Scheme 1d).[9–12] Due to the steric repulsion between the exocyclic auxiliaries and the central (dihydro)anthracene-type core, the quinodimethane form **V-A** and the biradical form **V-B** adopt significantly different geometries (folded and twisted shapes, respectively) because the deformation mode, which is suitable to reduce steric repulsion, is different depending on the double- or single-bond character of the exocyclic bonds in **V-A** and **V-B**, respectively.

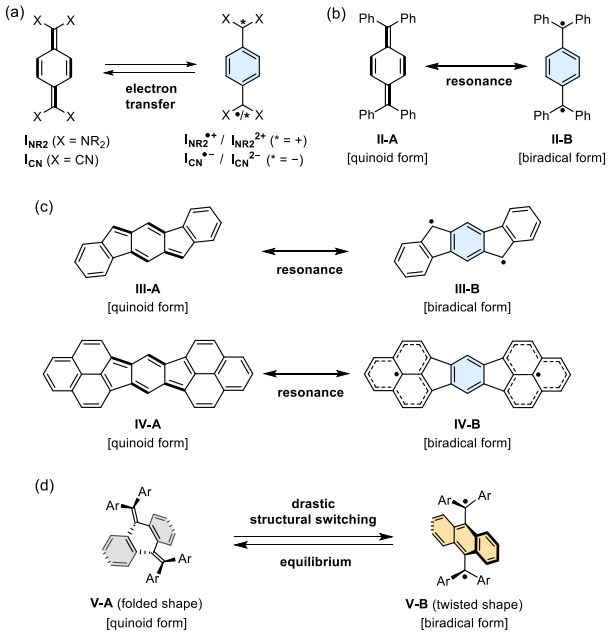

Scheme 1. (a) Structural switching upon electron transfer, (b,c) almost no geometrical change by resonance structure, and (d) drastic structural switching based on a thermal equilibrium.

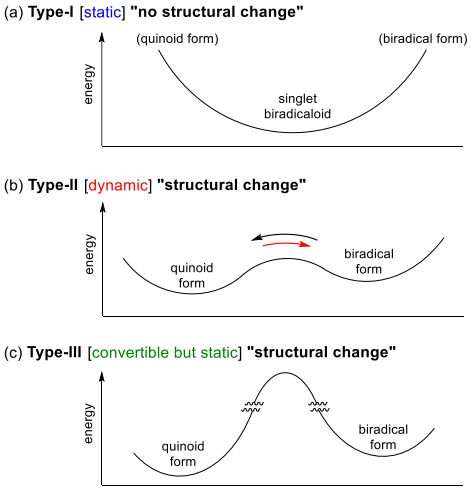

Scheme 2. Three types of quinodimethane-based biradicals/biradicaloids.

[a] Prof. Dr. Y. Ishigaki, S. Mizuno, Dr. K. Sugawara, T. Hashimoto, Prof. Dr. T. Suzuki
Department of Chemistry, Faculty of Science
Hokkaido University
Sapporo 060-0810 (Japan)
E-mail: yishigaki@sci.hokudai.ac.jp; tak@sci.hokudai.ac.jp
[b] Prof. Dr. S. Suzuki
Graduate School of Engineering Science
Osaka University
Osaka 560-8531 (Japan)

Supporting information for this article is given via a link at the end of the document.

While the closed-shell quinoid form (**A**) and the open-shell biradical form (**B**) are formulated as resonance pairs in singlet biradicaloids [Type-I] for **II**-**IV**, anthraquinodimethane (**V**-**A**) and anthracene-9,10-diyl (**V**-**B**) are completely different species based on a drastic change in the structure, and thus they are shown to be in equilibrium while interconverting with a certain energy barrier for changes in their geometrical and electronic structures.[13] A few previous papers[14,15] have reported successful isolation of both the closed-shell quinoid form (**V**-**A**) and the open-shell biradical form (**V**-**B**), in which light irradiation or heating at high temperature was used to overcome the large energy barrier to trigger interconversion [Type-III ($\Delta G^{\ddagger}$ > 25 kcal mol^{-1})] (Scheme 2).

There is another situation for **V**-**A** and **V**-**B**, so that they can coexist in an equilibrium while they are interconverting rapidly, even at ambient temperature, thanks to the small energy barrier for interconversion [Type-II ($\Delta G^{\ddagger}$ < 15 kcal mol^{-1})]. Here we report the first series of compounds of the Type-II category, based on the anthraquinodimethane skeleton attached to methoxyphenylthienyl groups (e.g., **1**, Scheme 3), and clarify the conditions to be fulfilled during the molecular design.[16] The fast interconversion between the closed-shell quinoid form (**A**) and the open-shell biradical form (**B**) provides Type-II systems with dynamic properties, such as temperature-dependent redox behavior,[13] which cannot be realized in molecules of Type-I (static system) or Type-III (convertible but static system).

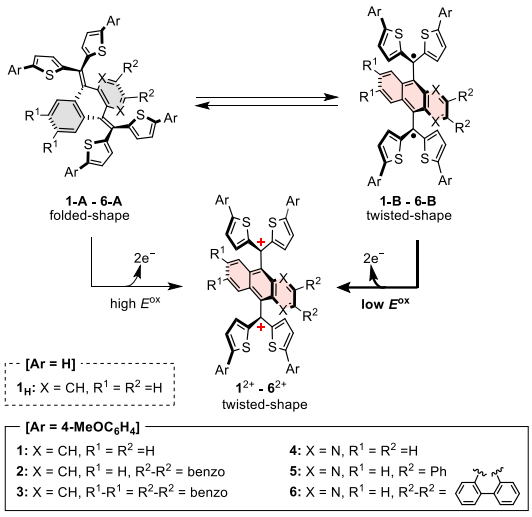

Scheme 3. Redox-active anthraquinodimethanes **1**−**6** with thienyl groups.

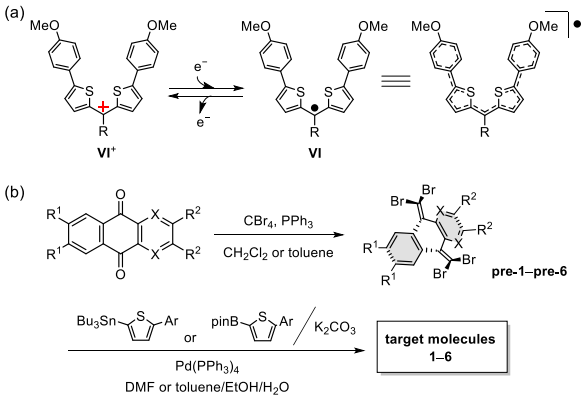

Scheme 4. (a) Redox interconversion of extended cyanine dye **VI**$^{+}$. (b) Preparation of target anthraquinodimethanes **1**−**6** via cross-coupling reactions using bis(dibromomethylene) derivatives **pre**-**1**−**pre**-**6**.

Results and Discussion

Molecular Design.

Type-I and Type-III are two extreme cases in terms of the relationship between the closed-shell quinoid form (**A**) and the open-shell biradical form (**B**). In Type-I, no geometrical change should occur for these two resonance structures. In contrast, in Type-III, the two forms have quite different geometrical and electronic structures. A bulky and rigid tricyclic subunit, such as fluorenyl,[17,18] dimethyldihydroanthryl,[14] or dialkoxythioxanthenyl,[15] on each end of the exocyclic bonds provides a high enough energy barrier ($\Delta G^{\ddagger}$ > 25 kcal mol^{-1}) to suppress mutual interconversion under ambient conditions. These features of the subunit also fulfill the requirement to stabilize the biradical forms (**B**) by steric protection with suppressing the side reactions of the open-shell species in Type-III molecules.

For the molecular design of Type-II, steric protection of the open-shell species (**B**) should not be adopted by considering that it may hamper rapid equilibrium with the closed-shell state (**A**). Thus, the radical subunits on the exocyclic bonds should be stabilized by delocalization of the spin over the extended π-system. Indeed, we have demonstrated that there is a thermal equilibrium between anthraquinodimethane **1**-**A** and biradical **1**-**B**, which was designed as a prototype of the Type-II family. Additionally, we recently disclosed that bis[5-(4-methoxyphenyl)-2-thienyl]methyls (**VI**) can serve as a series of stable neutral radicals with delocalization of spin over its completely planar skeleton, which were readily generated by one-electron (1e) reduction of extended cyanine dye salts (**VI**$^{+}$BF$_4^{-}$) (Scheme 4a).[19]

By considering that 2-thienyl groups on the exocyclic carbons exhibit moderate steric repulsion with the central core, the closed-shell quinoid form **1**-**A** would adopt a folded shape. On the other hand, open-shell biradical form **1**-**B** would have a planar central core of anthracene, to which two stable radical units are attached at the 9,10-positions in a nearly perpendicular manner. π-Extension by attachment of the methoxyphenyl substituent at the 5-position of the 2-thienyl group is essential since an unsubstituted 2-thienyl group was found to be less effective for stabilizing the biradical state thermodynamically.[13]

In this context, to achieve coexistence of the closed-shall quinoid form (**A**) and the open-shell biradical form (**B**), the energy difference between the two states [ΔG^{o} = G^{o} (**B**) - G^{o} (**A**)] should be small. This value is largely affected by the substituents on the thienyl groups as shown above. At the same time, ΔG^{o} would also be changed by modifying the central core. Thus, tetracene and pentacene derivatives (**2** and **3**) are included in this study. These higher acene analogues would exhibit a greater preference for the closed-shell quinoid form (**2**-**A** and **3**-**A**), due to less gain of aromatic stabilization in the central core upon conversion to **2**-**B** and **3**-**B** than to **1**-**B**. Further modification of the central core by incorporating two nitrogen (N) atoms at the *peri*-positions is planned, so that a fused pyrazine ring in **4** acts as a platform for diphenyl substitution (as in **5**) or for phenanthrene annulation (as in **6**). Such a slight perturbation would help us to estimate the limiting value of ΔG^{o} to behave as a Type-II system. The compound with a central core with four N atoms is not included in this work, since tetraaryltetraazaanthraquinodimethanes were recently shown to have such a flexible geometry that they can adopt several kinds of closed-shell conformations;[20] thus, dynamic interconversion with the biradical form would be too complicated for analysis.

Preparation and Structural Features of 1−6.

As in the cases of other tetraarylanthraquinodimethanes,[9–12,17,21–23] the target compounds were readily prepared from the corresponding bis(dibromomethylene) derivatives **pre-1**−**pre-6** via Pd(0)-catalyzed cross-coupling reactions using 2-(4-methoxyphenyl)-5-tributylstannylthiophene[13] or 5-(4-methoxyphenyl)-2-thienylboronic acid pinacol ester.[19] The precursors **pre-1**−**pre-6** were obtained by treating the corresponding quinones with CBr_4 and PPh_3 (Scheme 4b).[23–26] All of the new compounds **1** - **6** were obtained as stable yellow solids, for which a vapor diffusion method gave single-crystalline samples suitable for X-ray analyses.

As shown in Figures 1 and S12, all of the compounds adopt similar folded geometries. Thus, they exist as the folded-shaped quinoid form **1-A**−**6-A** in the solid state, suggesting that the closed-shell quinoid form is more stable than the open-shell biradical form **1-B**−**6-B**. This assumption is in accord with the theoretical estimation of ΔE by DFT calculations [(U)CAM-B3LYP/6-31G*] as shown later. Upon treatment of CH_2Cl_2 solutions of **1-A**, **2-A**, and **6-A** with two equivalents of (4-$BrC_6H_4)_3N^{+\bullet}SbCl_6^-$ (Magic Blue), the dication salts $\mathbf{1}^{2+}(SbCl_6^-)_2$, $\mathbf{2}^{2+}(SbCl_6^-)_2$, and $\mathbf{6}^{2+}(SbCl_6^-)_2$ were obtained quantitatively, the X-ray structures of which showed a perpendicularly twisted structure for the dicationic species (Figure 2).

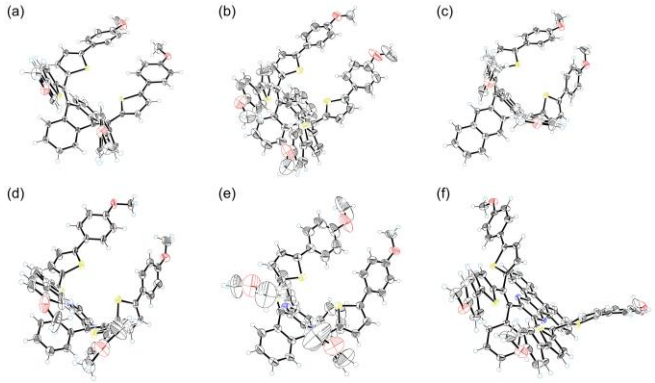

Figure 1. X-ray structures of (a) **1-A**$^{\#}$ (CCDC 1971277),[13] (b) **2-A**$^{\#}$, (c) **3-A**$^{\#}$, (d) **4-A**$^{\#}$, (e) **5-A**$^{\#}$, and (f) **6-A**$^{\#}$ measured at 150 K. Disordered atoms are omitted for clarity. Thermal ellipsoids are shown at the 50% probability level. $^{\#}$One of the two (**1-A**, **2-A**, **4-A**, and **5-A**), three (**6-A**) or four (**3-A**) crystallographically independent molecules is shown.

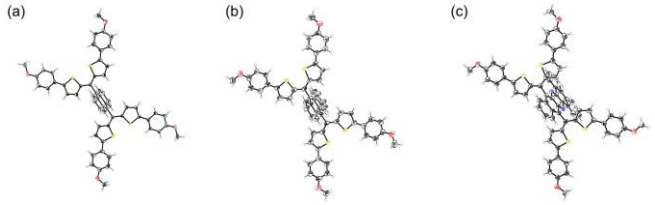

Figure 2. X-ray structures of dications in (a) $\mathbf{1}^{2+}(I_3^-)_2$ (CCDC 1971278),[13] (b) $\mathbf{2}^{2+}(SbCl_6^-)_2$, and (c) $\mathbf{6}^{2+}(SbCl_6^-)_2$ salts measured at 150 K. The counterions and disordered atoms are omitted for clarity. Thermal ellipsoids are shown at the 50% probability level.

Despite the fact that the molecular geometries of these dications ($\mathbf{1}^{2+}$, $\mathbf{2}^{2+}$, and $\mathbf{6}^{2+}$) are similar to the assumed twisted geometries of the open-shell biradical forms (**1-B**, **2-B**, and **6-B**), reduction of the dication salts with Zn powder did not generate the open-shell biradicals but rather quantitatively gave the solids, which were identical to those of the closed-shell quinoid forms (**1-A**, **2-A**, and **6-A**). This outcome is quite different from that with the Type-III compounds, for which, upon reduction of the twisted dications, the twisted biradical forms (**B**) were generated and kinetically trapped without converting to the corresponding quinoid forms (**A**) because of the suitably high energy barrier ($\Delta G^{\ddagger}$).[15] Thus, the newly prepared **1-6** were shown to not belong to the Type-III category, which prompted us to further study the present molecules to investigate if they are Type-II compounds that undergo rapid equilibrium with partial conversion of the quinoid form (**A**) to the open-shell biradical form (**B**).

Thermal Equilibrium of 1-A and 1-B, and Negligible Contributions from 2-B and 3-B.

When crystals of **1-A** were dissolved in CD_2Cl_2, its ^{1}H NMR spectrum exhibited a set of sharp resonances at 193 K assignable to the C_{2v}-symmetric folded form, which was determined by X-ray analysis. With an increase in the temperature, all of the resonances became broad, suggesting a partial conversion of **1-A** to the thermally excited triplet biradical form **1-B** (Figure 3). A variable-temperature (VT) analysis was also conducted for the electron spin resonance (ESR) measurement in CH_2Cl_2 (Figure S40a). At 303 K, a strong signal assignable to **1-B** was observed; its intensity decreased upon cooling, and finally the signal almost disappeared at 193 K. The ESR spectrum in a frozen solution of benzophenone at 233 K is that for the typical triplet species. From the zero-field splitting parameter D, the spin-separation distance was estimated to be 8.0 Å by the point-dipole approximation, which fits the geometry of a twisted biradical form of **1-B**. The observed change in the contribution of the biradical form with an increase in temperature is a characteristic feature of Type-II compounds. Based on the above results, we concluded that **1-A**/**1-B** is the first Type-II compound that interconverts rapidly between the most stable quinoid form (**A**) and the metastable biradical form (**B**). Notably, the equilibrated mixture of **1-A** and **1-B** in a solution can be handled under air and ambient conditions without any special precaution, thanks to the persistence of the neutral radical skeletons in **1-B**.

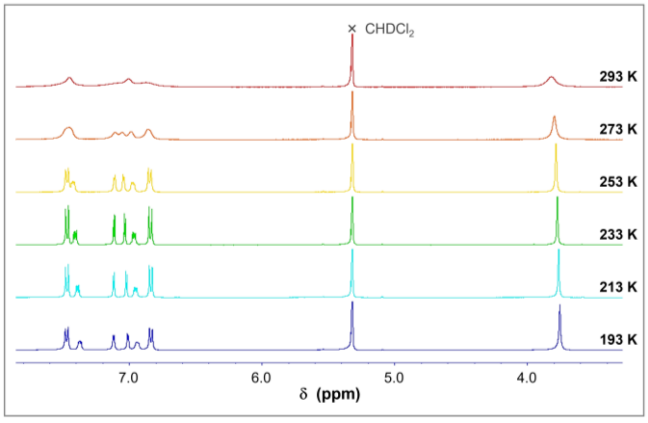

Figure 3. VT-^{1}H NMR spectra of **1** in CD_2Cl_2, showing a decrease in the contribution from triplet biradical **1-B** at lower temperatures.

To generate a certain population of the biradical form (**B**) in the equilibrated mixture, the 4-methoxyphenyl group at the 5-position of the 2-thienyl group in **1** plays an important role, as revealed by spectral studies for tetra(2-thienyl)anthraquinodimethane $\mathbf{1_H}$,[13] in which all of the four 4-methoxyphenyl groups are removed. Thus, the ^{1}H NMR spectrum of $\mathbf{1_H}$ in $CDCl_3$ showed sharp resonances at ambient temperature, and no signal was observed when the ESR measurement was conducted under conditions similar to those of **1-A**/**1-B** (Figure S40b).

Both the substituents on the 2-thienyl groups and the annulation of benzene rings at the central core affect the population of the biradical form (**B**). Thus, tetracenequinodimethane **2** and pentacenequinodimethane **3** exhibited sharp resonances in their ^{1}H NMR spectra, which were assignable to their folded forms **2**-**A** and **3**-**A**, respectively. Even when their DMSO-d_6 solutions were heated to 393 K (Figure S41), no change was observed in the spectrum of **3**-**A** while two independent resonances for the MeO groups of **2**-**A** at different chemical shifts ($\Delta\delta$ = 0.029 ppm, $\Delta\nu$ = 11.6 Hz at 303 K) were merged at the coalescence temperature (T_c) of 353 K, from which the energy barrier was deduced to be 18.5 kcal mol^{-1} for rotation of the exocyclic bonds in **2**-**A**.

Density Functional Theory (DFT) Calculations for the Energy Differences and Energy Barriers for 1−3 and Related Compounds.

Spectral studies on **1**−**3** and **1$_H$** showed that **1** has a small energy difference (ΔG^o) between the most stable quinoid form **1**-**A** and the metastable biradical form **1**-**B**. Facile interconversion of **1**-**A** and **1**-**B** indicated by the continuous changes in the VT-ESR spectrum supported this small energy barrier ($\Delta G^‡$). Small ΔG^o and $\Delta G^‡$ values are prerequisites for compounds that belong to Type-II, and **1**-**A**/**1**-**B** fulfill these conditions. On the other hand, the relative energies of the biradical forms **2**-**B**, **3**-**B** and **1$_H$**-**B** were suggested to be too high to make measurable contributions in the equilibrated mixtures. These considerations prompted us to conduct a series of DFT calculations [(U)CAM-B3LYP/6-31G*] (Table 1), and their optimized structures for both quinoid forms (**A**) and biradical forms (**B**) are summarized in Figures S12-S14.

Both the quinoid form (**A**) and the biradical form (**B**) were optimized as the energy-minimized geometries for **1**−**3** and **1$_H$**. For the biradicals of **1**-**B**−**3**-**B** and **1$_H$**-**B**, the singlet-triplet energy gaps ($\Delta E_{s\text{-}t}$) were shown to be very small (–0.07 - 0 kcal mol^{-1}) for all cases. This can be explained by considering the nearly identical geometries of the present biradicals irrespective of the spin state (singlet or triplet) as well as the very weak inter-spin interaction due to separation by the central aromatic core, which is attached perpendicularly to the radical centers. Thus, the energy differences (ΔE) were shown to indicate the differences between the biradical form of the triplet state and the singlet quinoid form in the following text.

From the viewpoint of a change in geometry, the interconversion between the quinoid form (**A**) with a folded shape and the biradical form (**B**) with a twisted shape would proceed through the transition state (TS) with a closed-shell twisted geometry, which is less-perpendicular than the corresponding biradical form. DFT calculations also gave the energy for the TS in each pair, which is also given in Table 1. The estimated small energy barrier for **1** (15.0 kcal mol^{-1}) suggests that interconversion between **1**-**A** and **1**-**B** could not be suppressed at ambient temperature. The energy of the TS coincides with the energy barrier for the rotation of exocyclic bonds in the quinoid form (**A**), and the experimental value of **2**-**A** (18.1 kcal mol^{-1}) was well reproduced by the calculated $\Delta G^‡$ (17.1 kcal mol^{-1}) at the CAM-B3LYP/6-31G* level.

By comparing the values in Table 1, the different spectral features among **1**-**3** could be explained by the larger ΔE for the higher-acene analogues of **2**-**A**/**2**-**B** (8.11 kcal mol^{-1}) and **3**-**A**/**3**-**B** (16.1 kcal mol^{-1}), thus diminishing the contribution from biradicals **2**-**B** and **3**-**B** upon dissolution of the crystals of the quinoid forms **2**-**A** and **3**-**A**. In this way, **2** and **3** were shown to be closed-shell molecules without any contribution from the corresponding biradicals under the experimentally attainable conditions. Similar suppression of biradical contribution was previously reported for derivatives of bis(9-fluorenyl)anthracene biradical,[18] benzannulation to which caused a preference for the corresponding quinoid forms.

The calculated energy difference for **1**-**A**/**1**-**B** (1.07 kcal mol^{-1}) indicates that there is only a limited contribution from **1**-**B** in the equilibrated mixture (Table 1). On the other hand, when additional calculations were conducted at the (U)B3LYP/6-31G* level, the stability of biradical forms was overestimated,[13] and the biradical form **1**-**B** was predicted to be more stable than the quinoid form **1**-**A**, which is against the experimental observation of the VT-ESR measurement. Thus, further discussion in this paper will be conducted based on theoretically calculated values at the (U)CAM-B3LYP/6-31G* level.

Different Degrees of the Copresence of the Quinoid Form and the Biradical Form in Diaza-analogues 4−6.

Compound **4** has a structure in which two CH groups at the *peri*-positions of **1** are replaced by N atoms. This modification facilitates rotation of the exomethylene bonds compared to **1**-**A** due to less steric hindrance. Thus, the $\Delta G^‡$ value for interconversion between **4**-**A**−**6**-**A** and **4**-**B**−**6**-**B** would be smaller than that for **1**-**A**/**1**-**B**. Among **4**−**6**, the π-extension of the central core is largest in **6** with a dibenzodiazatetracene skeleton, so that ΔG^o between the quinoid form (**A**) and biradical form (**B**) would be largest in **6**, with a decrease in the contribution from **6**-**B**. Investigation of a series of compounds with a subtle change in structure (e.g., **5** versus **6**) should provide useful information on the requisites for Type-II behavior.

Figure 4a shows the ESR spectra of **4**, **5**, and **6** in fluid solution at 303 K prepared by dissolving crystals of **4**-**A**, **5**-**A**, and **6**-**A** (2 mM each) in CH_2Cl_2. The ESR spectrum of the sample prepared from **6**-**A** exhibited the absence of signal (ESR silent), while those prepared from **4**-**A** and **5**-**A** showed clear peaks (ESR active). The ESR-active spectra revealed the presence of the triplet state of biradicals **4**-**B** and **5**-**B** which were generated from the thermal equilibrium conversion of the quinoid forms **4**-**A** and **5**-**A**, respectively. Validation of the triplet species was accomplished by ESR spectroscopy of **4**-**B** and **5**-**B** in frozen solutions of benzophenone at 233 K (Figures 4b and S40c). VT-ESR measurements in CH_2Cl_2 revealed a decline in signal intensity with a decrease in temperature, indicative of a reduced population of biradicals **4**-**B** and **5**-**B** at lower temperatures (Figure 4c,d). Although the signal intensity is weaker in diphenyl-substituted **5**-**B** than in **4**-**B**, ESR studies demonstrated that diaza-analogues **4**-**A**/**4**-**B** and **5**-**A**/**5**-**B** are also Type-II compounds.

In accord with the ESR spectral features, the ^{1}H NMR spectra of CD_2Cl_2 solutions obtained by dissolving **4**-**A**, **5**-**A**, and **6**-**A** crystals are different from each other. At 293 K, the spectrum of the solution of **6**-**A** exhibited sharp resonances whereas those of **4**-**A** and **5**-**A** were featureless or broadened, indicating the presence of a certain amount of triplet biradicals **4**-**B** and **5**-**B** in the latter two. With a decrease in temperature, the ^{1}H NMR spectra of **4**-**A**/**4**-**B** and **5**-**A**/**5**-**B** gradually sharpened, as expected (Figure S42). VT-NMR analyses were also conducted for **6**-**A**. The spectrum exhibited continuous changes upon cooling, corresponding to the suppression of exomethylene rotation while giving an energy barrier of 12.2 kcal mol^{-1} based on the coalescence temperature (T_c = 240 K) and chemical shift difference ($\Delta\nu$ = 18.7 Hz at 193 k) between two methoxy proton signals (Figure S43). This small value supports fast equilibrium between the quinoid form **6**-**A** and the biradical form **6**-**B**,

however, the silent ESR spectrum as well as sharp NMR resonances of a solution of **6**-**A** show that the contribution from biradical **6**-**B** is negligibly small, probably due to a larger energy difference (ΔG^{o}) than for **4**-**B** and **5**-**B**.

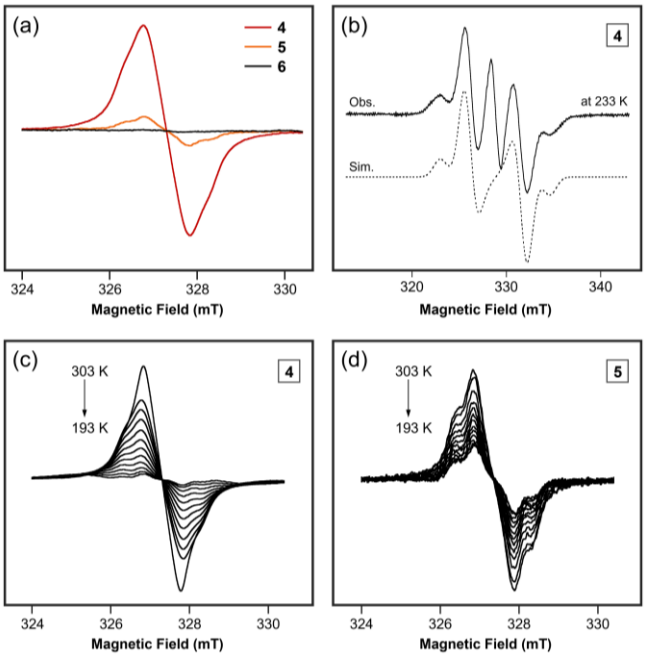

and (d) **5-A**/**5-B** measured in CH_2Cl_2 (2 mmol L^{-1}) at 303 K-193 K.

DFT Calculations of Energy Differences and Energy Barriers for Diaza-analogues 4−6.

To account for the different behaviors among **4**−**6**, DFT calculations were conducted [(U)CAM-B3LYP/6-31G*] (Table 1). In accord with the spectroscopic data, the energy differences of **4**-**A**/**4**-**B** and **5**-**A**/**5**-**B** (ΔE: 3.19 and 3.63 kcal mol^{-1}, respectively) were slightly higher than that of **1**-**A**/**1**-**B** (1.07 kcal mol^{-1}). Considering that the value for **6**-**A**/**6**-**B** was estimated to be 4.09 kcal mol^{-1}, the calculated ΔE value should be in the range of 1-4 kcal mol^{-1} for coexistence of the quinoid form (**A**) and the biradical form (**B**) to behave as Type-II compounds, so that the metastable biradical form of the triplet state could be detected by ESR and NMR spectroscopy.

In terms of the energy barrier ($\Delta G^{\ddagger}$) for interconversion between the quinoid form (**A**) and the biradical form (**B**) for these diaza derivatives **4**−**6**, the calculated values are lower (< 10 kcal mol^{-1}) than that of **1**-**A**/**1**-**B** (15.0 kcal mol^{-1}), and thus, replacing two C-H groups by N atoms in the central core part effectively lowers the $\Delta G^{\ddagger}$ value. Notably, the calculated value for **6**-**A**/**6**-**B** (8.08 kcal mol^{-1}) is close to the experimentally determined energy barrier for rotation of the exocyclic bonds in **6**-**A** (6.93 kcal mol^{-1}). These results indicate that, to achieve Type-II behavior, a smaller $\Delta G^{\ddagger}$ value for the change in structure between the form **A**/**B** is quite important, e.g., a value of 15.0 kcal mol^{-1} is enough to realize rapid equilibrium in solution at ambient temperature.

Table 1. Calculated relative energies (ΔE) of quinoid (**A**) and biradical (**B**) forms.[a]

Compds. (central core)	quinoid (**A**) singlet	biradical (**B**) singlet[b]	biradical (**B**) triplet[b]	transition state[c]
1 (anthracene)	0	+1.07	+1.07	+15.0
2 (tetracene)	0	+8.11	+8.11	+17.1
3 (pentacene)	0	+16.1	+16.1	+20.6
4 (diazaanthracene)	0	+3.18	+3.19	+9.29
5 (Ph_2-diaza-anthracene)	0	+3.63	+3.63	+7.75
6 (dibenzodiaza-tetracene)	0	+4.09	+4.09	+8.08
$\mathbf{1_H}$ (anthracene)	0	+4.33	+4.33	+16.8

[a] Values in kcal mol^{-1} calculated by a DFT method at (U)CAM-B3LYP/6-31G* level. The calculated ΔE values are used in the text for discussing ΔG°. [b] Calculations for the geometry with two S atoms facing each other, which is a more stable conformation than other conformers in biradical form (**B**). [c] The optimized structure adopts a closed-shell twisted geometry, which corresponds to the transition state (negative frequency) for the interconversion between the quinoid form (**A**) and the biradical form (**B**).

Redox Properties of Type-II Compounds.

Due to the coexistence of the quinoid form (**A**) and the biradical form (**B**), Type-II compounds essentially can exhibit redox properties corresponding to both forms. At the same time, electrochemical measurements often exhibit only the behavior corresponding to the more redox-active species [e.g., the biradical form (**B**)] because of the rapid interconversion. In this way, even when the biradical form (**B**) exists in a very small proportion, the voltammogram looks as if all of the molecules adopt the biradical form.

For the typical Type-II compounds **1**, **4**, and **5**, the voltammograms in CH_2Cl_2 exhibited a pair of reversible waves corresponding to two-electron (2e) transfer at +0.30, +0.29, and +0.30 V vs SCE, respectively, at 297 K with a scan rate of 100 mV s^{-1} (Figure 5 and Table 2). By considering that the dications have a geometry with a planar central core, to which two diarylmethylium units are attached nearly perpendicularly (Figure 2), the reversible nature clearly shows that the redox-active species in solutions of **1**, **4**, and **5** are the biradical forms (**1**-**B**, **4**-**B**, and **5**-**B**) with geometries quite similar to those of the corresponding dications. The one-wave 2e-transfer could be explained by supposing that the two radical units or the two cation units behave almost independently. Although the calculation indicated that the biradical forms (**B**) are minor components in the equilibrated mixtures, the voltammograms of **1**, **4**, and **5** at 297 K only showed peaks corresponding to the more easily oxidizable biradical forms **1**-**B**, **4**-**B**, and **5**-**B** because they were supplied by fast interconversion from the folded forms **1**-**A**, **4**-**A**, and **5**-**A**, respectively.

On the other hand, the voltammograms of tetracenequinodimethane **2** and pentacenequinodimethane **3** showed that the cathodic peaks ($E_p^{cathode}$: +0.33 V and +0.30 V, respectively) are largely shifted from the corresponding anodic peaks (E_p^{anode}: +0.97 V and +0.95 V, respectively) (Figure 5). Such a separation of redox waves is characteristic of “dyrex” systems,[1] in which the oxidizable species (e.g., the quinoid form with a folded geometry) and the reducible species (e.g., the dication with a twisted geometry) adopt quite different structures. Thus, electrochemical studies also confirmed that there is no

contribution of the biradical form (**2**-**B** or **3**-**B**) due to large ΔG^{o} and $\Delta G^{\ddagger}$ values.

The above explanation could be further confirmed by conducting voltammetric analyses at low temperature where the equilibration between the folded form (**A**) and the biradical form (**B**) needs a longer time in response to the $\Delta G^{\ddagger}$ value. Under the same ΔG^{o} value, the metastable form becomes less populated at lower temperature. Thus, the voltammogram of **1** at 195 K exhibits a large separation of redox peaks (Figure 6 and Table 2), which is far different from that measured at 297 K but similar to those of **2** and **3** at ambient temperature. This observation could be accounted for by considering the suppression of interconversion from **1**-**A** to **1**-**B**, so that the voltammogram exhibited the oxidation peak of the less easily oxidizable quinoid form **1**-**A** (E_p^{anode}: +1.05 V). After oxidation, the resulting dication $\mathbf{1}^{2+}$ adopts a twisted geometry, and thus the return peak ($E_p^{cathode}$: +0.16 V) appeared at a potential similar to that measured at 297 K. The less effect of lowering the temperature for the voltammogram of **4** can be explained by the much smaller $\Delta G^{\ddagger}$ value than that of **1**, so that the interconversion between **4**-**A** and **4**-**B** is still fast at 195 K (Figure 6).

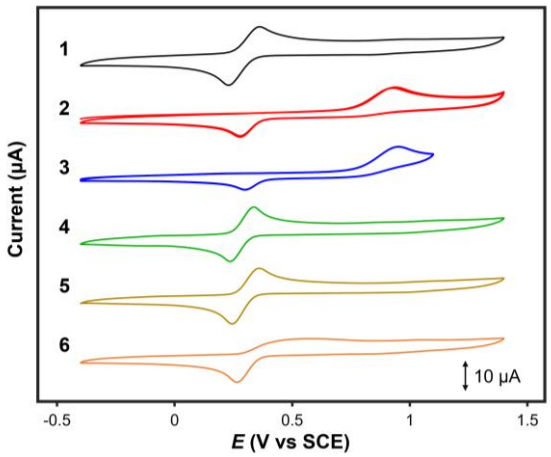

Figure 5. Cyclic voltammograms of $\mathbf{1}/\mathbf{1}^{2+}$, $\mathbf{2}/\mathbf{2}^{2+}$, $\mathbf{3}/\mathbf{3}^{2+}$, $\mathbf{4}/\mathbf{4}^{2+}$, $\mathbf{5}/\mathbf{5}^{2+}$, and $\mathbf{6}/\mathbf{6}^{2+}$ at 297 K in CH_2Cl_2 containing 0.1 mol L^{-1} Bu_4NBF_4 as a supporting electrolyte (*E*/V vs SCE, Pt electrode, scan rate 100 mV s^{-1}).

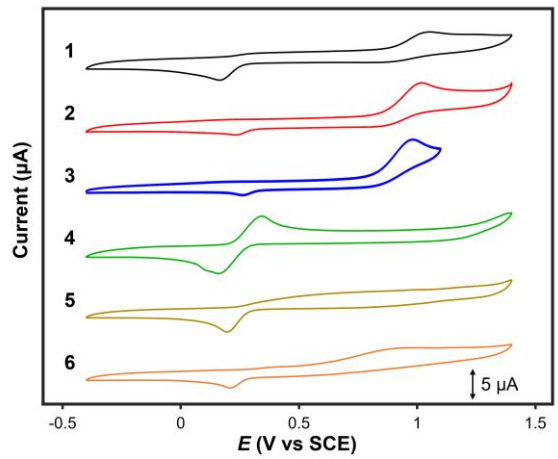

Figure 6. Cyclic voltammograms of $\mathbf{1}/\mathbf{1}^{2+}$, $\mathbf{2}/\mathbf{2}^{2+}$, $\mathbf{3}/\mathbf{3}^{2+}$, $\mathbf{4}/\mathbf{4}^{2+}$, $\mathbf{5}/\mathbf{5}^{2+}$, and $\mathbf{6}/\mathbf{6}^{2+}$ at 195 K in CH_2Cl_2 containing 0.1 mol L^{-1} Bu_4NBF_4 as a supporting electrolyte (*E*/V vs SCE, Pt electrode, scan rate 100 mV s^{-1}).

Table 2. Redox potentials measured in CH_2Cl_2 containing 0.1 M Bu_4NBF_4.[a]

	measured at 297 K			measured at 195 K	
Compds.	$E_{1/2}^{red}$	$E_p^{cathode}$	E_p^{anode}	$E_p^{cathode}$	E_p^{anode}
$\mathbf{1}^{2-}/\mathbf{1}/\mathbf{1}^{2+}$	−1.05	$E_{1/2}^{ox}$ = +0.30		+0.16	+1.05
$\mathbf{2}/\mathbf{2}^{2+}$	-	+0.33	+0.97	+0.22	+1.06
$\mathbf{3}/\mathbf{3}^{2+}$	-	+0.30	+0.95	+0.25	+1.00
$\mathbf{4}^{2-}/\mathbf{4}/\mathbf{4}^{2+}$	−1.09	$E_{1/2}^{ox}$ = +0.29		+0.16	+0.34
$\mathbf{5}^{2-}/\mathbf{5}/\mathbf{5}^{2+}$	−1.09	$E_{1/2}^{ox}$ = +0.30		+0.20	+0.73
$\mathbf{6}/\mathbf{6}^{2+}$	-	+0.27	+0.56	+0.21	+0.96

[a] Values in V vs SCE. [b] For the irreversible waves, peak potentials are shown as E_p^{anode} and $E_p^{cathode}$. All redox waves correspond to the 2e-processes.

When the electrochemical analyses of **1** were conducted at different temperatures between 195 K and 297 K, the voltammograms exhibited a continuous change between the two extreme cases: nearly reversible redox waves around +0.3 V at 297 K, and the two redox peaks being largely separated at 195 K. At intermediate temperatures, the anodic peak was broadened, which could be explained by supposing the oxidation of both less easily oxidizable species **1**-**A** and more easily oxidizable species **1**-**B** (Figure 7). Notably, the voltammogram of **5** at 195 K and those of **6** at 297 K and 195 K exihibited such broadening of the anodic peak, which means that those voltammograms show the oxidation processes of both the quinoid form (**5**-**A** or **6**-**A**) and the biradical form (**5**-**B** or **6**-**B**).

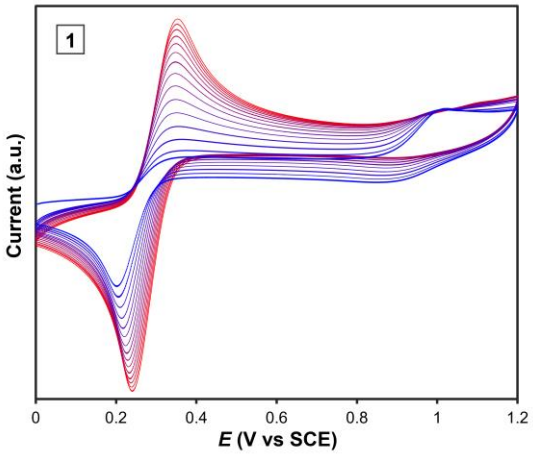

Figure 7. Cyclic voltammograms of $\mathbf{1}/\mathbf{1}^{2+}$ measured at various temperatures between 195 K and 297 K in CH_2Cl_2 containing 0.1 mol L^{-1} Bu_4NBF_4 as a supporting electrolyte (*E*/V vs SCE, Pt electrode, scan rate 100 mV s^{-1}).

Based on spectral studies showing no ESR signal and sharp ^1H NMR resonances for solutions obtained by dissolving **6**-**A** crystals, one can expect that the voltammogram of **6** is similar to those of **2** and **3** with a large separation of redox peaks. However, the broadened and less positive anodic peak in the voltammograms of **6** indicated the presence of a marginal but non-negligible amount of the biradical form **6**-**B** in the solution obtained by dissolving **6**-**A** crystals. Actually, when a solution of **6**-**A** in CH_2Cl_2 was treated with iodine (3 equiv.), dicationic salt $\mathbf{6}^{2+}(I_3^-)_2$ was obtained in 97% yield. The reaction with such a weak oxidant clearly showed the presence of the biradical form **6**-**B** in equilibrium, since a similar oxidation was observed for the

Type-II compound **1**-**A**/**1**-**B**, which allowed the isolation of $\mathbf{1}^{2+}(I_3^-)_2$ salt in 97% yield.[13] To detect formation of the biradical in equilibrium, the higher sensitivity of voltammetric analysis than of ESR or NMR spectrocopy was also suggested previously.[15]

Finally, another facet of Type-II compounds was disclosed by further voltammetric analyses of **1**, **4**, and **5**: i.e., very high electrochemical amphotericity (Scheme 5). Each of the biradical forms **1**-**B**, **4**-**B**, and **5**-**B** has two units of bis[5-(4-methoxyphenyl)2-thienyl]methyl moiety (as in **VI**), which undergoes 1e oxidation and reduction to the corresponding cationic and anionic states. For those biradicals, two radical units behave independently upon electron transfer, so that both redox waves in the voltammograms are 2e processes (Figure 8 and Table 2) that give the span of the second oxidation and reduction potentials E_2^{sum} (= E_2^{ox} - E_2^{red}) of 1.35, 1.38, and 1.39 V, respectively, which are record-small values for reversible 2e-processes.[27–34] By considering that similar amphotericity is not expected for the corresponding quinoid form (**A**) with much higher E^{ox} and much lower E^{red}, thermal control of the redox properties, especially such amphotericity with the smallest E_2^{sum} value, is the outstanding feature of Type-II molecules for developing highly functionalized materials.

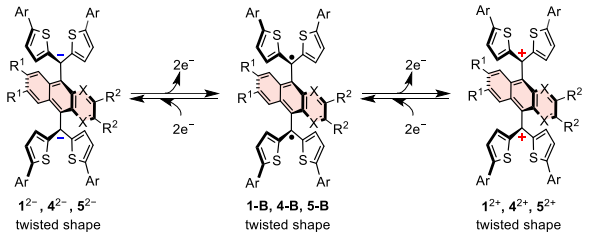

Scheme 5. Three-state redox interconversion based on electrochemical amphotericity of the biradical form of **1**-**B**, **4**-**B**, and **5**-**B**.

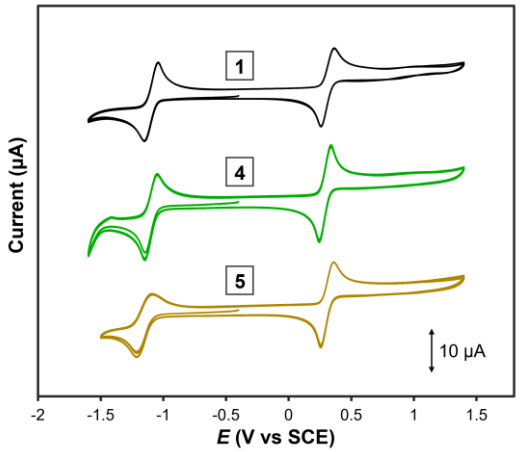

Figure 8. Cyclic voltammograms of $\mathbf{1}^{2-}$/**1**-**B**/$\mathbf{1}^{2+}$, $\mathbf{4}^{2-}$/**4**-**B**/$\mathbf{4}^{2+}$, and $\mathbf{5}^{2-}$/**5**-**B**/$\mathbf{5}^{2+}$ measured at 297 K in CH_2Cl_2 containing 0.1 mol L^{-1} Bu_4NBF_4 as a supporting electrolyte (*E*/V vs SCE, Pt electrode, scan rate 100 mV s^{-1}).

Conclusion

By the proper modification of tetraarylanthraquinodimethane **V**-**A**, dibenzo analogues of Thiele's hydrocarbon **II**, both the quinoid form (**A**) and the biradical form (**B**), with different geometries can coexist in solution with rapid equilibrium when the energy difference ΔG^o (1-4 kcal mol^{-1}) as well as the energy barrier for interconversion $\Delta G^{\ddagger}$ (< 15 kcal mol^{-1}) are small enough. The 5-(4-methoxyphenyl)2-thienyl groups on the exocyclic bond as well as the anthracene/diazaanthracene-type central core are suitable subunits to fulfill the conditions for ΔG^o and $\Delta G^{\ddagger}$. Thus, three entities of compounds (**1**, **4** and **5**) are the first members that allow the two forms to coexist in solution with fast equilibration, for which the population of metastable biradical forms (**B**) decreases with a decrease in temperature as demonstrated by VT-ESR measurements that exhibited ON-OFF switching of the magnetic properties. In electrochemical studies on the equilibrated mixtures in solution, the biradical forms **1**-**B**, **4**-**B** and **5**-**B** were shown to be highly redox-active compared to the quinoid form **1**-**A**, **4**-**A** and **5**-**A**, while exihibiting outstanding electrochemical amphotericity due to the open-shell character. Despite the limited population of the biradical form (**B**), the voltammogram at a higher temperature appeared as if all of the molecules exist as the biradical form, due to rapid conversion from the quinoid form (**A**). Because the temperature is the important factor for controlling the proportion of the two forms and the interconversion speed between them, the redox properties of **1**, **4** and **5** can be switched by temperature. The above properties, in combination with adequate chemical stability with no need for precautions in handling, show that molecules that undergo easy interconversion between the quinoid form (**A**) and the biradical form (**B**) can serve as a new class of organic molecules, which could be used for the future development of functional and switchable materials.

Experimental Section

General

All reactions were carried out under an argon atmosphere. All commercially available compounds were used without further purification. Dry toluene was obtained by distillation from CaH_2 prior to use. Column chromatography was performed on silica gel 60N (KANTO KAGAKU, spherical neutral) of particle size 40-50 μm or Wakogel® 60N (neutral) of particle size 38-100 μm. ^1H and ^{13}C NMR spectra were recorded on a BRUKER Ascend™ 400 (^1H/400 MHz and ^{13}C/100MHz) spectrometer at 296 K unless otherwise indicated. ESR spectra were recorded on a JEOL JES-FE2XG spectrometer. The samples for ESR measurements in fluid solution were prepared by dissolving the crystals **4**-**A**, **5**-**A**, and **6**-**A** in CH_2Cl_2, which were degassed by the freeze-pump-thaw method and then sealed before measurements. The samples for the ESR measurements for **4** and **5** in frozen-solution state were prepared as follows: A mixture of the compound (3 wt%) and benzophenone was placed in an ESR tube. The ESR tube was degassed under reduced pressure and sealed. The tube was heated to 333 K to obtain the sample of a melted-benzophenone solution. Subsequently, it was rapidly cooled to 233 K to afford a frozen solution state. IR spectra were measured by using the attenuated total reflection (ATR) mode on a Shimadzu IRAffinity-1S ATR/IR spectrophotometer. Mass spectra were recorded on a JMS-T100GCV spectrometer in FD mode or a Q Exactive Plus in ESI positive mode by Dr. Eri Fukushi and Mr. Yusuke Takata (GS-MS & NMR Laboratory, Research Faculty of Agriculture, Hokkaido University). Melting points were measured on a Yamato MP-21 or on a Stanford Research Systems OptiMelt MPA100 and are uncorrected. Elemental analyses were performed on an EXETER ANALYTICAL CE440 or a MICRO CORDER JM10 at the Center for Instrumental Analysis of Hokkaido University. UV/Vis/NIR spectra were recorded on a JASCO V-770 spectrophotometer. Redox potentials (E^{ox} and

E^{red}) were measured on a BAS ALS-612EX by cyclic voltammetry in dry CH_2Cl_2 containing 0.1 M Bu_4NBF_4 as a supporting electrolyte. All of the values shown in the text are in *E*/V vs. SCE measured at the scan rate of 100 mVs^{-1}. Pt electrodes were used as the working (disk) and counter electrodes. The working electrode was polished using a water suspension of aluminum oxide (0.05 μm) before use. DFT calculations were performed with the Gaussian 16W program package.[35] The geometries of the compounds were optimized by using the CAM-B3LYP method in combination with the 6-31G* basis set unless otherwise indicated. A suitable crystal was selected and measured on a Rigaku XtaLAB Synergy (Cu-Kα radiation, λ = 1.54184 Å) with HyPix diffractometer. The crystal was kept at 150 K during data collection. Using Olex2,[36] the structure was solved with the SHELXT[37] structure solution program using Intrinsic Phasing and refined with the SHELXL[38] refinement package using Least Squares minimization. Details of synthetic procedures are shown in the Supporting Information.

Supporting Information

The authors have cited an additional reference within the Supporting Information.[39]

Acknowledgements

This work was supported by Grant-in-Aid from MEXT and JSPS (Nos. JP20H02719 to T.S. and JP21H01912 and JP23H04011 to Y.I.). Y.I. acknowledges JST PRESTO (No. JPMJPR23Q1). This work was also supported by the "Five-star Alliance" in "NJRC Mater. & Dev." MEXT.

Keywords: Cations • Electrochemical amphotericity • Radicals • Thermal equilibrium

[1] Y. Ishigaki, K. Sugawara, T. Tadokoro, Y. Hayashi, T. Harimoto, T. Suzuki, *Chem. Commun.* **2021**, *57*, 7201–7214.
[2] A. Maiti, S. Chandra, B. Sarkar, A. Jana, *Chem. Sci.* **2020**, *11*, 11827–11833.
[3] D. S. Acker, W. R. Hertler, *J. Am. Chem. Soc.* **1962**, *84*, 3370–3374.
[4] Z. Pei, N. L. Magann, M. J. Sowden, R. B. Murphy, M. G. Gardiner, M. S. Sherburn, M. L. Coote, *J. Am. Chem. Soc.* **2023**, *145*, 16037–16044.
[5] J. Thiele, H. Balhorn, *Berichte der Dtsch. Chem. Gesellschaft* **1904**, *37*, 1463–1470.
[6] C. K. Frederickson, B. D. Rose, M. M. Haley, *Acc. Chem. Res.* **2017**, *50*, 977–987.
[7] T. Kubo, *Chem. Lett.* **2015**, *44*, 111–122.
[8] T. Kubo, *Bull. Chem. Soc. Jpn.* **2021**, *94*, 2235–2244.
[9] Y. Ishigaki, K. Sugawara, M. Yoshida, M. Kato, T. Suzuki, *Bull. Chem. Soc. Jpn.* **2019**, *92*, 1211–1217.
[10] Y. Sakano, R. Katoono, K. Fujiwara, T. Suzuki, *Chem. Lett.* **2014**, *43*, 1143–1145.
[11] Z. He, L. Zhang, J. Mei, T. Zhang, J. W. Y. Lam, Z. Shuai, Y. Q. Dong, B. Z. Tang, *Chem. Mater.* **2015**, *27*, 6601–6607.
[12] X. Zhang, X. Jiang, K. Zhang, L. Mao, J. Luo, C. Chi, H. S. O. Chan, J. Wu, *J. Org. Chem.* **2010**, *75*, 8069–8077.
[13] A part of this paper was published as a preliminary communication: Y. Ishigaki, T. Hashimoto, K. Sugawara, S. Suzuki, T. Suzuki, *Angew. Chem. Int. Ed.* **2020**, *59*, 6581–6584.
[14] T. Nishiuchi, R. Ito, E. Stratmann, T. Kubo, *J. Org. Chem.* **2020**, *85*, 179–186.
[15] M. B. S. Wonink, B. P. Corbet, A. A. Kulago, G. B. Boursalian, B. de Bruin, E. Otten, W. R. Browne, B. L. Feringa, *J. Am. Chem. Soc.* **2021**, *143*, 18020–18028.
[16] Y. Ishigaki, T. Harimoto, T. Shimajiri, T. Suzuki, *Chem. Rev.* **2023**, *123*, 13952–13965.
[17] Z. Zeng, Y. M. Sung, N. Bao, D. Tan, R. Lee, J. L. Zafra, B. S. Lee, M. Ishida, J. Ding, J. T. López Navarrete, Y. Li, W. Zeng, D. Kim, K.-W. Huang, R. D. Webster, J. Casado, J. Wu, *J. Am. Chem. Soc.* **2012**, *134*, 14513–14525.
[18] X. Yin, J. Z. Low, K. J. Fallon, D. W. Paley, L. M. Campos, *Chem. Sci.* **2019**, *10*, 10733–10739.
[19] S.-G. Chong, S. Suzuki, T. Suzuki, Y. Ishigaki, *Bull. Chem. Soc. Jpn.* **2023**, *96*, 1144–1149.
[20] K. Sugawara, T. Ono, Y. Yano, T. Suzuki, Y. Ishigaki, *Mater. Chem. Front.* **2023**, *7*, 1591–1598.
[21] M. Desroches, P. Mayorga Burrezo, J. Boismenu-Lavoie, M. Peña Álvarez, C. J. Gómez-García, J. M. Matxain, D. Casanova, J.-F. Morin, J. Casado, *Angew. Chem. Int. Ed.* **2017**, *56*, 16212–16217.
[22] T. Nishiuchi, S. Aibara, H. Sato, T. Kubo, *J. Am. Chem. Soc.* **2022**, *144*, 7479–7488.
[23] T. Suzuki, Y. Umezawa, Y. Sakano, H. Tamaoki, R. Katoono, K. Fujiwara, *Chem. Lett.* **2015**, *44*, 905–907.
[24] R. Neidlein, M. Winter, *Synthesis (Stuttg).* **1998**, *1998*, 1362–1366.
[25] Z. He, L. Shan, J. Mei, H. Wang, J. W. Y. Lam, H. H. Y. Sung, I. D. Williams, X. Gu, Q. Miao, B. Z. Tang, *Chem. Sci.* **2015**, *6*, 3538–3543.
[26] C.-Y. Chiu, B. Kim, A. A. Gorodetsky, W. Sattler, S. Wei, A. Sattler, M. Steigerwald, C. Nuckolls, *Chem. Sci.* **2011**, *2*, 1480–1486.
[27] K. Nakasuji, K. Yoshida, I. Murata, *J. Am. Chem. Soc.* **1982**, *104*, 1432–1433.
[28] T. Kubo, K. Yamamoto, K. Nakasuji, T. Takui, I. Murata, *Bull. Chem. Soc. Jpn.* **2001**, *74*, 1999–2009.
[29] K. Nakasuji, T. Kubo, *Bull. Chem. Soc. Jpn.* **2004**, *77*, 1791–1801.
[30] X. Guégano, A. L. Kanibolotsky, C. Blum, S. F. L. Mertens, S. Liu, A. Neels, H. Hagemann, P. J. Skabara, S. Leutwyler, T. Wandlowski, A. Hauser, S. Decurtins, *Chem. – A Eur. J.* **2009**, *15*, 63–66.
[31] X. Shi, E. Quintero, S. Lee, L. Jing, T. S. Herng, B. Zheng, K.-W. Huang, J. T. López Navarrete, J. Ding, D. Kim, J. Casado, C. Chi, *Chem. Sci.* **2016**, *7*, 3036–3046.
[32] Q. Jiang, Y. Han, Y. Zou, H. Phan, L. Yuan, T. S. Herng, J. Ding, C. Chi, *Chem. – A Eur. J.* **2020**, *26*, 15613–15622.
[33] H. Hayashi, J. E. Barker, A. Cárdenas Valdivia, R. Kishi, S. N. MacMillan, C. J. Gómez-García, H. Miyauchi, Y. Nakamura, M. Nakano, S. Kato, M. M. Haley, J. Casado, *J. Am. Chem. Soc.* **2020**, *142*, 20444–20455.
[34] G. I. Warren, L. J. Zocchi, L. N. Zakharov, M. M. Haley, *Chem. – A Eur. J.* **2023**, *29*, e202301153.
[35] M. J. Frisch, G. W. Trucks, H. B. Schlegel, G. E. Scuseria, M. A. Robb, J. R. Cheeseman, G. Scalmani, V. Barone, G. A. Petersson, X. Nakatsuji, H.; Li, M. Caricato, A. V. Marenich, J. Bloino, B. G. Janesko, R. Gomperts, B. Mennucci, H. P. Hratchian, J. V. Ortiz, A. F. Izmaylov, J. L. Sonnenberg, D. Williams-Young, F. Ding, F. Lipparini, F. Egidi, J. Goings, B. Peng, A. Petrone, T. Henderson, D. Ranasinghe, V. G. Zakrzewski, J. Gao, N. Rega, G. Zheng, W. Liang, M. Hada, M. Ehara, K. Toyota, R. Fukuda, J. Hasegawa, M. Ishida, T. Nakajima, Y. Honda, O. Kitao, H. Nakai, T. Vreven, K. Throssell, J. A. J. Montgomery, J. E. Peralta, F. Ogliaro, M. J. Bearpark, J. J. Heyd, E. N. Brothers, K. N. Kudin, V. N. Staroverov, T. A. Keith, R. Kobayashi, J. Normand, K. Raghavachari, A. P. Rendell, J. C. Burant, S. S. Iyengar, J. Tomasi, M. Cossi, J. M. Millam, M. Klene, C. Adamo, R. Cammi, J. W. Ochterski, R. L. Martin, K. Morokuma, O. Farkas, J. B. Foresman, D. J. Fox, *Gaussian 16, Revision B.01*, Gaussian, Inc., Wallingford CT, 2016, **n.d.**
[36] O. V. Dolomanov, L. J. Bourhis, R. J. Gildea, J. A. K. Howard, H. Puschmann, *J. Appl. Crystallogr.* **2009**, *42*, 339–341.
[37] G. M. Sheldrick, *Acta Crystallogr. Sect. A Found. Adv.* **2015**, *71*, 3–8.
[38] G. M. Sheldrick, *Acta Crystallogr. Sect. C Struct. Chem.* **2015**, *71*, 3–8.
[39] G. A. Efimova, L. S. Efros, *Zh. Org. Khim.* **1966**, *2*, 531.
[40] Deposition numbers 1971277 (for **1**-**A**), 2335099 (for **2**-**A**), 2335100 (for **3**-**A**), 2335101 (for **4**-**A**), 2335102 (for **5**-**A**), 2335103 (for **6**-**A**), 1971278 (for $\mathbf{1}^{2+}(I_3^-)_2$), 2335104 (for $\mathbf{2}^{2+}(SbCl_6^-)_2$), and 2335105 (for $\mathbf{6}^{2+}(SbCl_6^-)_2$) contain the supplementary crystallographic data for this paper. These data are provided free of charge by the joint Cambridge Crystallographic Data Centre and Fachinformationszentrum Karlsruhe Access Structures service.

Entry for the Table of Contents

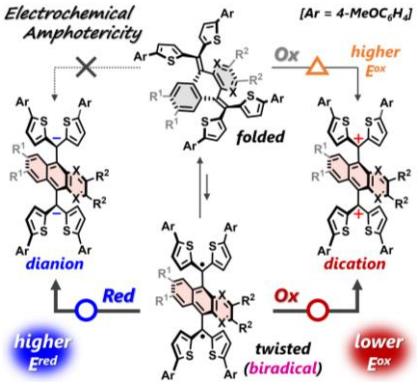

An open-shell biradical form, which is generated by a thermal equilibrium with the closed-shell quinoid form in solution, exhibits electrochemical amphotericity. For the biradicals, since two radical units behave independently upon electron transfer, both oxidation and reduction proceed in two-electron processes. As a result, these biradicals show an exceptionally small difference between second oxidation and second reduction potentials.

Institute and/or researcher Twitter usernames: Yusuke Ishigaki (@ysk_isgk), and Laboratory (@Yuuichi_Hokudai)